

# Electron heat diffusivity in radially-bounded ergodic region of toroidal plasma

Ryutaro Kanno<sup>1,2</sup>, Masanori Nunami<sup>1,2</sup>, Shinsuke Satake<sup>1,2</sup>,  
Seikichi Matsuoka<sup>3</sup>, and Hisanori Takamaru<sup>4</sup>

<sup>1</sup> National Institute for Fusion Science, National Institutes of Natural Sciences, Toki 509-5292, Japan

<sup>2</sup> Department of Fusion Science, SOKENDAI (The Graduate University for Advanced Studies), Toki 509-5292, Japan

<sup>3</sup> Japan Atomic Energy Agency, 178-4 Wakashiba, Kashiwa 277-0871, Japan

<sup>4</sup> Department of Computer Science, Chubu University, Kasugai 487-8501, Japan

E-mail: kanno@nifs.ac.jp

30 June 2017

**Abstract.** Drift-kinetic  $\delta f$  simulations are performed to investigate effect of ergodic field lines caused by resonant magnetic perturbations (RMPs) on radial heat diffusivity of electrons in the edge region of toroidal plasma of collisionality  $\nu_* \sim 0.1$ . The following is assumed in the simulations. The ergodic region is bounded radially on both sides by closed magnetic surfaces. The pressure gradient remains nonzero in the ergodic region because of an incomplete flattening of the pressure profile, and the characteristic scale length of the pressure gradient is of larger order than the overlapping width of the neighbouring magnetic islands. It is found in the quasi-steady state of  $\delta f$  that the electron heat diffusivity is of smaller order than the theoretical estimate derived by the Rechester-Rosenbluth model (Rechester A.B. and Rosenbluth M.N. 1978 *Phys. Rev. Lett.* **40** 38). The radial heat conduction is dominated not only by parallel motions along the ergodic field lines but also by trapped particle motions generated by the RMP field. The contribution of the trapped particles reduces the radial heat conduction enhanced by the parallel motions.

PACS numbers: 52.25.Fi, 52.65.Pp

*Keywords:* resonant magnetic perturbation, heat diffusion, drift-kinetic simulation  
Submitted to: *Nucl. Fusion*

## 1. Introduction

In recent tokamak experiments, resonant magnetic perturbations (RMPs) are used to suppress/mitigate edge localized modes (ELMs) in the plasma edge region of the collisionality  $\nu_* \sim 0.1$  [1, 2]. The definition of  $\nu_*$  is given in section 2. In the ELM suppression experiments [3, 4], it is found that the experimental estimate of the radial heat diffusivity of electrons affected by the RMPs is fairly small compared to the theoretical estimate derived by the Rechester-Rosenbluth (hereafter, R-R) model [5, 6]. On the other hand, if magnetic field lines affected by the RMPs become ergodic (or stochastic) and if the width of the ergodic region is approximately the same as the width of the edge region, the R-R model is considered to be applicable for estimating the heat diffusivity in the edge region. Applicability of the R-R model in the estimation of the diffusion coefficient was verified by a Monte Carlo simulation of guiding centre motions [7]. Therefore, there is an open question: why does there occur a difference between the theoretical results and the experimental results?

This question is composed of two parts. The first issue to be discussed is whether the RMP field penetrates the plasma in the ELM suppression experiments. This is not yet completely resolved at present. If the RMP field is screened by the plasma rotation [8], then field lines in the perturbed region do not become ergodic. As a result, the field-line diffusion given by the R-R model is not realised. However, the RMP penetration in the case of ELM mitigation is reported in magneto-hydrodynamic (MHD) simulation studies [8, 9, 10]. We assume in this paper that an ergodic region exists in the plasma edge region affected by the RMP field and is bounded radially on both sides by closed magnetic surfaces, and that good confinement in the plasma edge region is maintained in which the ELMs are suppressed. Note that in general, the heat confinement deteriorates if the ergodic region is not bounded radially and field lines in the ergodic region connect to the divertor target plates [11, 12]. The second issue is whether the field-line diffusion given by the R-R model is realised in such a radially-bounded ergodic region. The phenomenon in which ergodic field lines are confined in a finite domain plays an important role for the magnetic confinement of the toroidal plasma. That phenomenon is discussed showing the recent results in detail in [13]. For example, it is well known that guiding centre motions in the radially-bounded ergodic region differ from random motions given in the R-R model [14]. Therefore, if ergodic field lines are confined in the radially-bounded region and if the pressure gradient remains nonzero in the ergodic region because of an incomplete flattening of the pressure profile, there is a possibility that the radial heat diffusivity is different from the estimate of the R-R model.

Other possibilities may explain the difference between the theoretical results and the experimental results. Recently, the kinetic ion-electron-neutral guiding centre code XGC0, which is the kinetic simulation code for treating the so-called full distribution function (i.e., a full- $f$  simulation code), has been applied to the plasma transport in an ergodic region [15], where the screening of RMPs is not investigated. It is reported

that the electron heat transport is significantly reduced from the R-R model. In this simulation, many physical effects are considered. These include self-consistent radial electric field, Coulomb/neutral collisions, particle source from wall-recycling and neutral transport, electron cooling from the impurity radiation, and others. Thus, it is not clear whether the combination of many physical effects is essential for the explanation of the difference, or the difference is obtained in a simpler situation.

While drift-kinetic  $\delta f$  simulation [16, 17] is known to be a powerful tool for estimation of neoclassical transport in toroidal plasmas including 3-dimensional field geometry, the simulation code has rarely been used in studies of collisional transport in the ergodic region. When applying the drift-kinetic  $\delta f$  simulation code to the transport in the ergodic region, care should be taken that the presupposition  $|\delta f/f^{(0)}| \ll 1$  is required to be satisfied because the quadratic collision term  $C(\delta f, \delta f)$  is ignored in the simulation code, where  $f^{(0)}$  is the background distribution function given in advance in this paper. Here, the roles of  $f^{(0)}$  and  $\delta f$  are explained in section 2. In the previous work [18], we developed a drift-kinetic  $\delta f$  simulation code that includes the effect of the radial electric field in order to estimate the electron heat diffusivity in the ergodic region. However, the approach to the open question was insufficient because it was not clear which assumption is necessary for  $f^{(0)}$  satisfying  $|\delta f/f^{(0)}| \ll 1$ . In this paper, this point will be discussed. Then, in order to answer the second question, which is the key point in the open question raised in this paper, we will examine the effect of ergodic field lines on the radial heat diffusivity of electrons in the radially-bounded region using the drift-kinetic  $\delta f$  simulation under an assumption of zero electric field, which is the same assumption as provided in the R-R model. For the sake of a simpler comparison between the simulation and the R-R model, it is also assumed that effects of MHD activities, turbulence, mean flow, impurities, and neutrals are ignored. Because many physical effects are neglected, it is difficult to directly compare our simulation and the full- $f$  simulation. However, our simulation will show that the electron heat diffusivity is significantly reduced when compared to the R-R model in the simpler situation than the full- $f$  simulation.

This paper is organised as follows. In section 2, the ergodic region used in the simulations is briefly explained. The assumption for  $f^{(0)}$  satisfying  $|\delta f/f^{(0)}| \ll 1$  is discussed. The effect of ergodic field lines on the electron heat diffusivity is examined. The summary and discussions are given in section 3.

## 2. Drift-kinetic $\delta f$ simulations

### 2.1. Simulation model

In the  $\delta f$  Monte Carlo simulation code KEATS [18, 19], we introduce the following ordering into the representation of a distribution function  $f$  in the drift-kinetic equation:  $f = f^{(0)} + f^{(1)}$  and  $|f^{(1)}/f^{(0)}| \ll 1$ . Here, the 0th-order distribution function  $f^{(0)}$  is set to a Maxwellian  $f^{(0)} = f_M = n(m/2\pi T)^{3/2} \exp\{-m\mathbf{v}^2/2T\}$  with fixed profiles of

temperature  $T$  and number density  $n$ , where  $m$  is the particle mass,  $\mathbf{v}$  is the velocity, and the mean velocity is ignored. The 1st-order distribution function  $f^{(1)}$  is the difference from  $f_M$ , i.e.,  $f^{(1)} = \delta f = f - f_M$ . The temperature and the number density are assumed to be given functions of a label of reference surfaces, where the reference surfaces are defined by the unperturbed magnetic flux surfaces. Due to the presupposition  $|f^{(1)}/f^{(0)}| \ll 1$ , the drift-kinetic  $\delta f$  simulation is required to ensure that orders of characteristic scale lengths  $L^{(0)}$  and  $L^{(1)}$  of the 0th-order and the 1st-order distribution functions are well separated from each other, i.e.,  $L^{(1)}/L^{(0)} \ll 1$ . In this paper, the characteristic scale lengths  $L^{(0)}$  and  $L^{(1)}$  are estimated as  $L^{(0)} \sim \mathcal{O}(|\partial \ln T_e / \partial r|^{-1})$  and  $L^{(1)} \sim \mathcal{O}(W_{\text{island}})$ , where  $T_e$  is the electron temperature and  $W_{\text{island}}$  is the overlapping width of neighbouring magnetic islands. Note that the 0th-order distribution function  $f_M$  is characterised by the scale length of the temperature gradient because the gradient of the number density is set to be zero in the estimation of the electron heat diffusivity. On the other hand, the 1st-order distribution function  $\delta f$  is strongly affected by the scale length of the ergodic region, i.e.,  $W_{\text{island}}$ , as discussed below. Here, the ratio of the electron banana width  $\delta r_b^e$  to the overlapping width  $W_{\text{island}}$  is set to satisfy  $\delta r_b^e / W_{\text{island}} \ll 1$ , where  $\delta r_b^e$  is estimated as  $\delta r_b^e \sim \rho_p^e \sqrt{\epsilon_t}$ ,  $\rho_p^e$  is the electron poloidal gyroradius, and  $\epsilon_t^{-1}$  is the aspect ratio.

Applying the decomposition  $f = f_M + \delta f$  to the drift-kinetic equation in 5-dimensional phase space  $(\mathbf{x}, v_{\parallel}, v)$ , we have the following equation with respect to electrons confined in static magnetic field  $\mathbf{B}$ :

$$\frac{D}{Dt} \delta f = - \left\{ \frac{D}{Dt} f_M - C_F f_M \right\}, \quad (1)$$

where  $D/Dt := \partial/\partial t + \dot{\mathbf{x}} \cdot \partial/\partial \mathbf{x} + \dot{v}_{\parallel} \partial/\partial v_{\parallel} - C_T$ ,  $\dot{\mathbf{x}} = \mathbf{v} = v_{\parallel} \mathbf{b} + \mathbf{v}_d$ ,  $\dot{v} = 0$ ,  $v = |\mathbf{v}|$ , and  $\dot{v}_{\parallel} = -\{\mathbf{B}^* \cdot (\mu/m) \nabla B\} / B_{\parallel}^*$  [20, 21]. Here, the electric field  $\mathbf{E}$  is ignored and is set to  $\mathbf{E} = 0$ . The parallel and drift velocities are given as  $v_{\parallel} = v_{\parallel} \mathbf{B}^* / B_{\parallel}^*$  and  $\mathbf{v}_d = -\{(\mu/e) \mathbf{b} \times \nabla B\} / B_{\parallel}^*$ , respectively. The magnetic moment  $\mu$  is represented as  $\mu = mv_{\perp}^2 / 2B$ ,  $v_{\perp} = \sqrt{v^2 - v_{\parallel}^2}$ ,  $\mathbf{B}^* = \mathbf{B} - (mv_{\parallel}/e) \nabla \times \mathbf{b}$ ,  $B_{\parallel}^* = \mathbf{b} \cdot \mathbf{B}^*$ ,  $\mathbf{b} = \mathbf{B} / |\mathbf{B}|$ ,  $e$  is the elementary charge, and the electron mass is written by  $m$ . The energy is given as  $\mathcal{E} = (1/2)mv^2 = \text{constant}$  in the case of  $\mathbf{E} = 0$ . The Coulomb collision operator is described by  $C_T$  and  $C_F$ , where  $C_T$  represents the pitch-angle scattering operators of electron-electron and electron-ion [21], and  $C_F$  is the field-particle collision operator which ensures the local momentum conservation property for the electron-electron collision and is given in section 3.8 of [21]. The boundary condition of the simulation is that the test particles (i.e., the sample guiding-centres having the two weights in the Monte Carlo method [18]) are absorbed when arriving at the wall of the calculation box. In the electron transport simulations, the ion distribution function, which species is set to be proton, is assumed to be the Maxwellian with the same profiles of temperature and number density as the electron profiles because the condition of  $|f^{(1)}/f^{(0)}| \ll 1$  is also satisfied in the case of ion [19, 22]. Here, when seen by the electrons, the Maxwellian of the ions is approximately a delta function without the case that the ion temperature is significantly larger than the electron temperature. Thus,

the ion temperature is assumed to be equal to the electron temperature for the purpose of simplifying the simulation.

The magnetic configuration is set to a simple tokamak field affected by RMPs. The major radius of the magnetic axis is  $R_{\text{ax}} = 3$  m, the minor radius of the toroidal plasma is  $a = 1$  m, and the strength of the magnetic field on the magnetic axis is  $B_{\text{ax}} = 2.5$  T. The temperature profile is given as  $T_e = T_i = T(r) = T_{\text{ax}} - (T_{\text{ax}} - T_{\text{edge}})r/a$  and the number density  $n_e = n_i = n$  is assumed to be constant (i.e.,  $\nabla \ln n = 0$ ), where  $r = r(R, Z) = \sqrt{(R - R_{\text{ax}})^2 + Z^2}$  is the label of the reference surfaces in the cylindrical coordinates  $(R, \varphi, Z)$ . The reference surfaces are given by magnetic flux surfaces of a circular tokamak field  $\mathbf{B}_0$ . The unperturbed magnetic field  $\mathbf{B}_0 = B_{0R}\hat{R} + B_{0\varphi}\hat{\varphi} + B_{0Z}\hat{Z}$  is given by  $B_{0R} = -B_{\text{ax}}Z/qR$ ,  $B_{0\varphi} = -B_{\text{ax}}R_{\text{ax}}/R$ , and  $B_{0Z} = B_{\text{ax}}(R - R_{\text{ax}})/qR$  [23], where  $q$  is the safety factor given as  $q = 1.8 + 3.1(r/a)^4$ , and  $\hat{R}$ ,  $\hat{\varphi}$ , and  $\hat{Z}$  are the unit vectors in the  $R$ ,  $\varphi$ , and  $Z$  directions, respectively. The RMP field, which causes resonance with rational surfaces satisfying  $3 < q = k/\ell < 4$  and  $\ell = 2, 3, 4, 5, 6, 7$ , is given by a perturbation field  $\delta\mathbf{B} = \nabla \times (\alpha\mathbf{B}_0)$ , which is the same type of RMPs used in [7, 14]. Here, the function  $\alpha$  is used to represent the structure of the RMP field;  $\alpha(R, \varphi, Z) = \sum_{k,\ell} a_{k\ell}(r) \sin\{k\theta - \ell\varphi\}$ , where  $\tan\theta = \tan\theta(R, Z) = Z/(R - R_{\text{ax}})$ ,  $a_{k\ell} = A_{\text{RMP}} \exp\{-(r - r_{k\ell})^2/\Delta r^2\}$  with  $A_{\text{RMP}}/a = 2 \times 10^{-3}$ ,  $r = r_{k\ell}$  is the rational surface of  $q = k/\ell$ , and  $\Delta r$  is a small parameter controlling the width of the perturbation, which is set to  $\Delta r/a = 5 \times 10^{-2}$ . The total magnetic field  $\mathbf{B}$  is  $\mathbf{B} = \mathbf{B}_0 + \delta\mathbf{B}$ . The Poincaré plots of magnetic field lines affected by the RMP field and the reference surfaces in the calculation box are shown in figure 1. The Chirikov parameter, which is the indicator of the overlapping of two magnetic islands [13], is estimated as  $\sigma_{\text{Chir}} = (1/2)\{w^{(k/\ell)} + w^{(k'/\ell')}\}/\Delta r^{(k/\ell, k'/\ell')} \gtrsim 1$  around the centre of the ergodic region. Here,  $\Delta r^{(k/\ell, k'/\ell')}$  is the width of the neighbouring rational surfaces of  $q = k/\ell, k'/\ell'$ , and  $w^{(k/\ell)}$  is the width of the  $(k, \ell)$  component of the RMPs, where  $W_{\text{island}}/a \gtrsim w^{(k/\ell)}/a \sim 0.02$  because several magnetic islands overlap each other. Note that all of the parameters mentioned above are in an artificial device, but are set for the sake of simplicity for comparing the simulation and the R-R model.

The radial heat diffusivity of electrons,  $\chi_r^e$ , is effectively estimated by

$$\chi_r^e = -\frac{Q_r^e(r)}{n_e(r)\partial T_e(r)/\partial r} \quad (2)$$

under the conditions of  $n_e = \text{constant}$ , zero electric field, and zero mean flow, where  $Q_r^e(r)$  is the radial energy flux of electrons in a quasi-steady state of  $\delta f$ . In the simulations, the radial energy flux crossing a reference surface labeled by  $r$  is given as

$$Q_r^e(r) = \overline{\left\langle \int d^3v \frac{mv^2}{2} (\nabla r \cdot \mathbf{v}) \delta f \right\rangle}. \quad (3)$$

Here,  $\overline{\phantom{x}}$  means the time-average, and the averaging time is of the same order as the typical time scale of  $\delta f$ , i.e., the electron-electron and electron-ion collision times, which are  $\tau_{ee}$  and  $\tau_{ei}$ , respectively. The time-averaging is carried out after sufficient exposure

to the Coulomb collision. The average  $\langle \cdot \rangle$  is defined as  $\langle \cdot \rangle = (1/\delta\mathcal{V}) \int_{\delta\mathcal{V}} \cdot d^3x$ , where  $\delta\mathcal{V}$  is a small volume and lies between two neighbouring reference surfaces with volumes  $\mathcal{V}(r)$  and  $\mathcal{V}(r) + \delta\mathcal{V}$ . The effective heat diffusivity in equation (2) is interpreted as the radial energy diffusivity.

The statistical properties of guiding centre motions in the ergodic region bounded radially by closed magnetic surfaces have been discussed in [14]. The relation between the so-called subdiffusive behaviour of the guiding centres and the diffusivity given from the drift-kinetic equation has been studied in detail in [19]. The verification between the  $\delta f$  simulation and the R-R model has also been performed in [22]. Those discussions are not repeated here. Note that the Monte Carlo simulation of guiding centre motions in the previous works [7, 14] corresponds to solving only the left-hand side of equation (1), i.e.,  $D\delta f/Dt = 0$  and  $\delta f = \sum_j \delta(\mathbf{x} - \mathbf{x}_j(t)) \delta(\mathbf{v} - \mathbf{v}_j(t))$  under considering the Maxwellian background, where  $j$  means the number of a sample guiding-centre.

## 2.2. Simulation results

Using the  $\delta f$  simulation code based on equation (1), we estimate the effective heat diffusivity of electrons in the toroidal plasma affected by the RMPs. The effective heat diffusivity  $\chi_r^e$  in the perturbed region in the case of  $T_{\text{ax}} = 1.137$  keV,  $T_{\text{edge}} = 0.8T_{\text{ax}}$ , and  $n = \text{constant} = 1 \times 10^{19} \text{ m}^{-3}$  is shown in figure 2, where the collisionality  $\nu_*$  in the perturbed region is estimated as  $\nu_* \approx 0.1$ . In general, the collisionality  $\nu_*$  is defined as  $\nu_* = \nu qR/\epsilon_t^{3/2} v_{\text{th}}$ . In the simulations, the collision frequency  $\nu$  is estimated to be  $\nu \sim \nu_{\text{ei}} \sim \tau_{\text{ei}}^{-1}$ , the thermal speed  $v_{\text{th}}$  is given as  $v_{\text{th}} = \sqrt{2T/m}$ , and  $R \sim R_{\text{ax}}$ , where  $\nu_{\text{ei}}$  is the electron-ion collision frequency. The effective heat diffusivity  $\chi_r^e$  evaluated in the simulation is fairly small compared to  $\chi_r^{\text{RR}} = \sum_{k,\ell} \pi q R_{\text{ax}} v_{\text{th}} \langle |\delta B_{k,\ell}|^2 \rangle / |B_{\text{ax}}|^2$  given by the R-R model [5, 6], i.e.,  $\chi_r^e/\chi_r^{\text{RR}} \lesssim 10^{-6}$  at the centre of the ergodic region  $r/a \approx 0.8$ , where  $\delta B_{k,\ell}$  is the  $(k, \ell)$  component of  $\nabla r \cdot \delta \mathbf{B}$ . Note that in this case the perturbed region is ergodic within  $0.6 < r/a < 1.0$ , but a closed magnetic surface remains and divides the ergodic region, as shown in figure 1, and the simulation satisfies  $L^{(1)}/L^{(0)} \lesssim 1/10$ .

We confirm that  $|\langle \int d^3v \delta f \rangle / n| \lesssim 10^{-4}$  and  $|\langle \int d^3v (1/2)mv^2 \delta f \rangle / (3nT/2)| \lesssim 10^{-3}$  for all  $r$  after several collision times in the simulation. Here, the number of the test particles which are absorbed at the wall of the calculation box is less than  $5 \times 10^{-3} \%$  of the total amount ( $\approx 2.58 \times 10^8$ ), where the test particles are initially distributed to be randomly uniform in the region of  $r/a \leq 1$  and  $0 \leq \varphi < 2\pi$ . In particular, the effect of the RMPs on the temperature profile is estimated by

$$\delta T = \frac{1}{n} \left\langle \int d^3v \left\{ \frac{1}{3}mv^2 - T(r) \right\} \delta f \right\rangle. \quad (4)$$

The modified temperature profile  $T^{(0+1)} = T^{(0)} + \delta T$  agrees well with the original profile  $T^{(0)} = T(r) = T_{\text{ax}} - (T_{\text{ax}} - T_{\text{edge}}) r/a$ , as shown in figure 3a. Therefore, the presupposition of the  $\delta f$  method, i.e.,  $|\delta f/f_{\text{M}}| \ll 1$ , is appropriately fulfilled in this simulation. When the condition of  $L^{(1)}/L^{(0)} \lesssim 1/10$  is satisfied, the effective heat diffusivity  $\chi_r^e$  given by equation (2) is independent from the temperature gradient, as shown in figure 4. It is

also confirmed that the presupposition of the  $\delta f$  method gradually becomes not satisfied if  $L^{(1)}/L^{(0)} \rightarrow 1$ , e.g.,  $L^{(0)}$  changes to a smaller scale, which means a steeper temperature gradient, or  $L^{(1)}$  changes to a larger scale, which means a broader overlapping width of magnetic islands. For example, if  $L^{(1)}$  changes to be larger than in the case of figure 3a,  $T^{(0+1)}$  becomes clearly different from  $T^{(0)}$  and flattened, as shown in figure 3b. However,  $T^{(0)}$  is replaced by a more gentle profile such that the condition of  $L^{(1)}/L^{(0)} \ll 1$  is satisfied, and  $T^{(0+1)} \approx T^{(0)}$  is realised. See figure 3c.

In the ELM suppression experiments [3, 4], the collisionality regime in the plasma edge region is estimated as  $\nu_* \approx 0.05-1$ . As shown in figure 5, the result that  $\chi_r^e/\chi_r^{\text{RR}} \ll 1$  is not sensitive to the collisionality  $\nu_*$ , where  $\nu_*$  is set by changing the value of the constant number density. It is also shown that the electron heat diffusivity, which is effectively evaluated from the radial energy flux in equation (2), is almost independent from the collisionality  $\nu_* \approx 0.05-1$ .

While the effective heat diffusivity in equation (2), i.e., the radial energy diffusivity, is independent from the collisionality  $\nu_*$ , the ratio of the radial heat flux  $q_r$  to the radial energy flux  $Q_r$  increases as the collisionality increases,  $\nu_* \rightarrow 1$ , as shown in figure 6, where  $Q_r = q_r + (5/2)T\Gamma_r$ ,  $\Gamma_r$  is the radial particle flux, and  $q_r$  and  $\Gamma_r$  are estimated in the same manner as in equation (3). This result means that the radial heat conduction estimated by  $q_r/(n|\partial T/\partial r|)$  is weakened and, inversely, the radial particle diffusion estimated by  $\Gamma_r/(n|\partial \ln T/\partial r|)$  is strengthened, when the collisionality is lower. Here, in all cases in figure 6, the gradient of the number density is set to be zero and the temperature profile is  $T(r) = T_{\text{ax}} - (T_{\text{ax}} - T_{\text{edge}})r/a$  with  $T_{\text{ax}} = 1.137$  keV and  $T_{\text{edge}} = 0.8T_{\text{ax}}$ . Then, there is a new question: why does the radial heat conduction become weakened in the case of lower collisionality? It is naturally expected that the parallel motions of guiding centres along ergodic field lines enhance the radial heat conduction in the case of lower collisionality. In the simulation results, this tendency is confirmed, as shown by the open squares in figure 7. The contribution of the parallel motions is estimated as the contribution of untrapped particles to  $q_r$ , which is evaluated as the radial heat flux satisfying the condition of  $\kappa^2 > 1$ , where  $\kappa^2$  is the pitch angle parameter  $\kappa^2 = \{(1/2)mv^2 - \mu B_{\text{ax}}(1 - \epsilon_t)\}/2\mu B_{\text{ax}}\epsilon_t$  [21] and  $q_r = q_r(\kappa^2 > 1) + q_r(\kappa^2 \leq 1) > 0$  in all cases. The contributions of untrapped and trapped particles are represented as  $q_r(\kappa^2 > 1)$  and  $q_r(\kappa^2 \leq 1)$ , respectively. On the other hand, the contribution of trapped particles satisfying the condition of  $\kappa^2 \leq 1$  negatively enhances the radial heat conduction against the positive enhancement of the parallel motions, as shown by the closed squares in figure 7. The contribution of the trapped particles reduces the radial heat conduction enhanced by the parallel motions. Here, it is confirmed in the simulation that  $q_r = q_r(\kappa^2 \lesssim 1) > 0$  and  $q_r/Q_r \approx 1$  in the unperturbed magnetic field under the conditions of  $\nabla \ln n = 0$  and  $\nu_* \approx 0.1$ , which is the same result as in the neoclassical transport theory [21].

### 3. Summary and discussions

Using the drift-kinetic  $\delta f$  simulation code KEATS [18], we investigate the effect of ergodic field lines caused by resonant magnetic perturbations (RMPs) on radial heat diffusivity of electrons in the cases of the collisionality  $\nu_* \approx 0.05-1$ . The simulations are performed under the conditions in which the ergodic region is bounded radially on both sides by closed magnetic surfaces and the characteristic scale length of the pressure gradient  $L^{(0)}$  is of larger order than the overlapping width of the neighbouring magnetic islands  $L^{(1)}$ . Note that the characteristic scales of the 0th-order and the 1st-order distribution functions are well separated from each other in the simulations.

It is found in the quasi-steady state of  $\delta f$  that the electron heat diffusivity is of smaller order than the theoretical estimate derived by the Rechester-Rosenbluth (R-R) model [5, 6]. This result indicates that the electron heat diffusivity is significantly reduced when compared to the R-R model even in the simpler situation than the full- $f$  simulation of [15]. The contribution of the trapped particle motions generated by the RMP field reduces the radial heat conduction enhanced by the parallel motions along ergodic field lines. The radial heat conduction is dominated not only by the parallel motions but also by the trapped particle motions. When the collisionality is lower under the condition of  $\nabla \ln n = 0$ , it is also seen that the radial heat conduction estimated by  $q_r/(n|\partial T/\partial r|)$  becomes weakened, and that the radial particle diffusion estimated by  $\Gamma_r/(n|\partial \ln T/\partial r|)$  becomes strengthened. The electron transport properties mentioned above differ from the properties derived by the R-R model and its successor models, which are developed from the R-R model under the consideration of guiding centre motions in ergodic field lines [13] and are included in the modelling of  $D\delta f/Dt = 0$ . In conclusion, the radial heat diffusion given by the R-R model is not realised in the radially-bounded ergodic region in the cases of the collisionality  $\nu_* \approx 0.05-1$ .

In general, detailed properties of radial electron and ion transport in 3-dimensional geometry are determined under the ambipolar condition. In addition, dependence of the electron transport on the detailed structure of field lines in the perturbed region is not investigated in this paper. The mechanism of the negative enhancement of the trapped particles in the radially-bounded ergodic region is not yet clear. These topics are left as future issues.

### Acknowledgments

The computational simulations in this paper were conducted using the supercomputers ‘‘Plasma Simulator’’ at National Institute for Fusion Science (NIFS) and ‘‘Helios’’ at International Fusion Energy Research Centre-Computational Simulation Centre (IFERC-CSC). This work was performed with the support and under the auspices of the NIFS Collaborative Research Programs ‘‘NIFS15KNST076’’ and ‘‘NIFS17KNST109’’, and the IFERC-CSC project ‘‘PETAMP5’’.

## References

- [1] Evans T.E. *et al* 2004 *Phys. Rev. Lett.* **92** 235003
- [2] Hawryluk R.J. *et al* 2009 *Nucl. Fusion* **49** 065012
- [3] Evans T.E. *et al* 2006 *Nature Phys.* **2** 419
- [4] Canik J.M. *et al* 2010 *Nucl. Fusion* **50** 034012
- [5] Rechester A.B. and Rosenbluth M.N. 1978 *Phys. Rev. Lett.* **40** 38
- [6] Ghendrih Ph. *et al* 1996 *Plasma Phys. Control. Fusion* **38** 1653
- [7] Boozer A. and White R.B. 1982 *Phys. Rev. Lett.* **49** 786
- [8] Orain F. *et al* 2013 *Phys. Plasmas* **20** 102510
- [9] Bécoulet M. *et al* 2014 *Phys. Rev. Lett.* **113** 115001
- [10] Orain F. *et al* 2017 *Nucl. Fusion* **57** 022013
- [11] Morisaki T. *et al* 2003 *J. Nucl. Mater.* **313-316** 548
- [12] Jakubowski M.W. *et al* 2006 *Phys. Rev. Lett.* **96** 035004
- [13] Abdullaev S. 2014 *Magnetic Stochasticity in Magnetically Confined Fusion Plasmas* (Cham: Springer)
- [14] Maluckov A. *et al* 2003 *Physica A* **322** 13
- [15] Park G. *et al* 2010 *Phys. Plasmas* **17** 102503
- [16] Wang W.X. *et al* 1999 *Plasma Phys. Control. Fusion* **41** 1091
- [17] Brunner S. *et al* 1999 *Phys. Plasmas* **6** 4504
- [18] Kanno R. *et al* 2016 *Contrib. Plasma Phys.* **56** 592
- [19] Kanno R. *et al.* 2010 *Plasma Phys. Control. Fusion* **52** 115004
- [20] Littlejohn R.G. 1983 *J. Plasma Phys.* **29** 111
- [21] Helander P. and Sigmar D.J. 2002 *Collisional Transport in Magnetized Plasmas* (Cambridge: Cambridge Univ. Press)
- [22] Kanno R. *et al.* 2013 *Plasma Phys. Control. Fusion* **55** 065005
- [23] Wesson J. 2011 *Tokamaks* 4th edn (New York: Oxford Univ. Press)

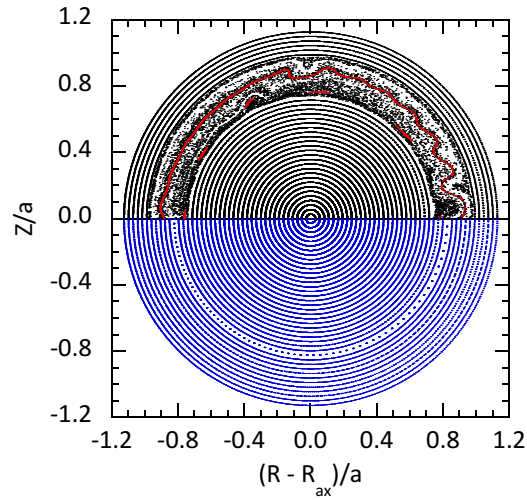


**Figure 1.** The upper half of this figure, which is illustrated in black, shows the Poincaré plots of magnetic field lines affected by the RMP field in the calculation box. In this case, a closed magnetic surface and a magnetic island remain in the perturbed region of  $0.6 < r/a < 1.0$ . These are shown in red for reference. The lower half of this figure, which is illustrated in blue, shows the reference surfaces given from the unperturbed magnetic field. Note that the calculation box includes the full torus.

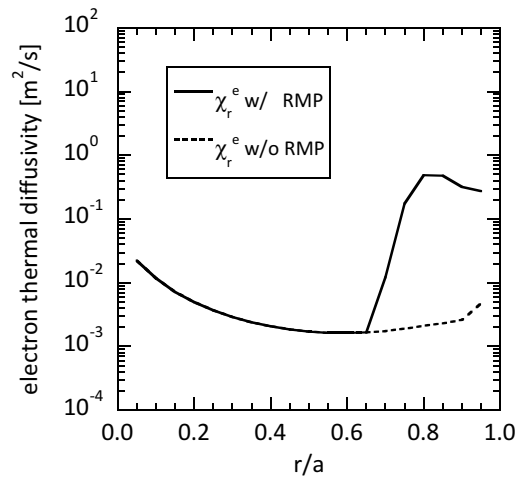


**Figure 2.** The effective heat diffusivity of electrons  $\chi_r^e$  is affected by the RMPs in  $0.6 < r/a < 1.0$ , as shown by the solid line. The value of the diffusivity affected by the RMPs at the centre of the ergodic region  $r/a \approx 0.8$  is a hundredfold larger than the neoclassical diffusivity illustrated by the dashed line, i.e.,  $\chi_r^e$  without RMP. Here, the temperature is set to  $T(r) = T_{\text{ax}} - (T_{\text{ax}} - T_{\text{edge}})r/a$  with  $T_{\text{ax}} = 1.137$  keV and  $T_{\text{edge}} = 0.8T_{\text{ax}}$ . The number density is  $n = \text{constant} = 1 \times 10^{19} \text{ m}^{-3}$ . The collisionality  $\nu_*$  is estimated as  $\nu_* \approx 0.1$  at  $r/a = 0.8$ .

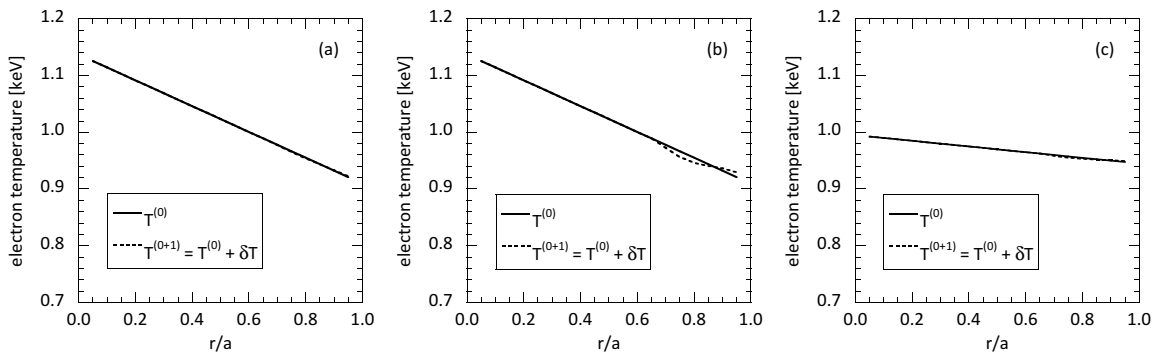


**Figure 3.** The original and modified temperature profiles  $T^{(0)}$  and  $T^{(0+1)} = T^{(0)} + \delta T$  are shown by the solid and dashed lines, respectively, where the perturbed region is set to be within  $0.6 < r/a < 1.0$ . (a) In the case of the simulation in figure 2, it is seen that  $T^{(0+1)} \approx T^{(0)}$ . (b)  $T^{(0)}$  is the same as in the case of (a).  $T^{(0+1)}$  is clearly different from  $T^{(0)}$ , where  $A_{\text{RMP}}/a = 2 \times 10^{-2}$  and  $1/10 \lesssim L^{(1)}/L^{(0)} < 1$ . (c)  $T^{(0)}$  is replaced by a more gentle profile satisfying  $L^{(1)}/L^{(0)} \ll 1$ , i.e.,  $T^{(0)} = T_{\text{ax}} - (T_{\text{ax}} - T_{\text{edge}})r/a$  with  $T_{\text{ax}} = 0.995$  keV and  $T_{\text{edge}} = 0.945$  keV. Then,  $T^{(0+1)} \approx T^{(0)}$  is realised. Here, the value of  $A_{\text{RMP}}/a$  is the same as in the case of (b).

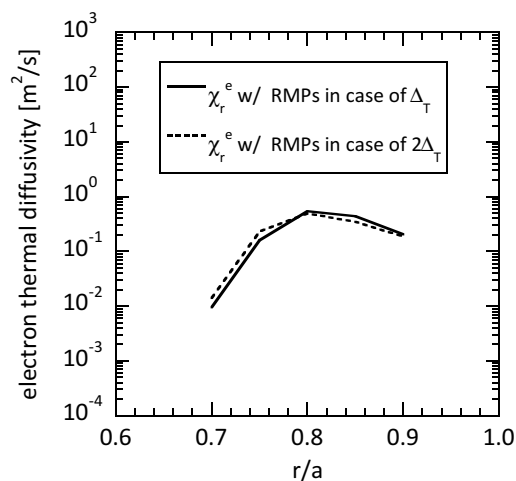


**Figure 4.** The effective heat diffusivity of electrons around the centre of the perturbed region  $r/a \approx 0.8$  does not substantially depend on the temperature gradient when the condition of  $L^{(1)}/L^{(0)} \lesssim 1/10$  is satisfied. Here, the temperature profile is given as  $T(r) = T_{\text{ax}} - (T_{\text{ax}} - T_{\text{edge}})r/a$  and the number density is fixed to be  $n = \text{constant} = 1 \times 10^{19} \text{ m}^{-3}$ . The simulation result in the case of  $T_{\text{ax}} = 1.137$  keV and  $T_{\text{edge}} = 0.8T_{\text{ax}}$  is shown by the solid line, which is the same as in figure 1. In this case, the temperature gradient is estimated as  $\Delta_T := |a \partial \ln T / \partial r| \approx 0.238$  at  $r/a = 0.8$ . The simulation result in the case of  $T_{\text{ax}} = 1.336$  keV and  $T_{\text{edge}} = 0.644T_{\text{ax}}$  is shown by the dashed line, where the temperature gradient is  $2\Delta_T$  at  $r/a = 0.8$ . Note that in both cases, the value of temperature at  $r/a = 0.8$  is set to be approximately 0.955 keV.

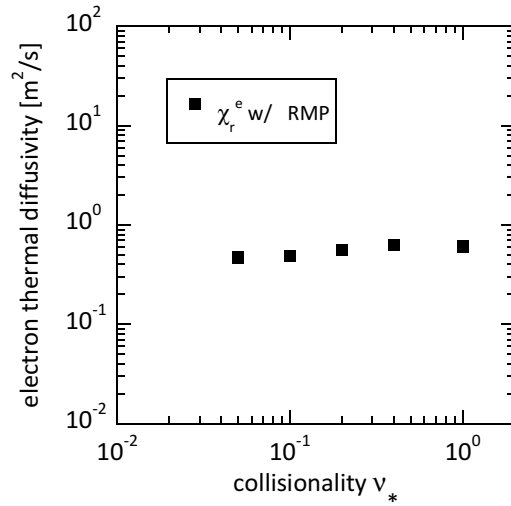


**Figure 5.** Dependence of the effective heat diffusivity of electrons  $\chi_r^e$  on the collisionality  $\nu_*$  is investigated in the radially-bounded ergodic region, where  $\chi_r^e$  is evaluated at  $r/a = 0.8$ . The diffusivity affected by the RMPs is almost independent from the collisionality  $\nu_*$  when  $\nu_* \approx 0.05-1$ , as shown by the closed squares. In all cases, the temperature profile is set to  $T(r) = T_{\text{ax}} - (T_{\text{ax}} - T_{\text{edge}})r/a$  with  $T_{\text{ax}} = 1.137$  keV and  $T_{\text{edge}} = 0.8T_{\text{ax}}$  and the gradient of the number density is zero.

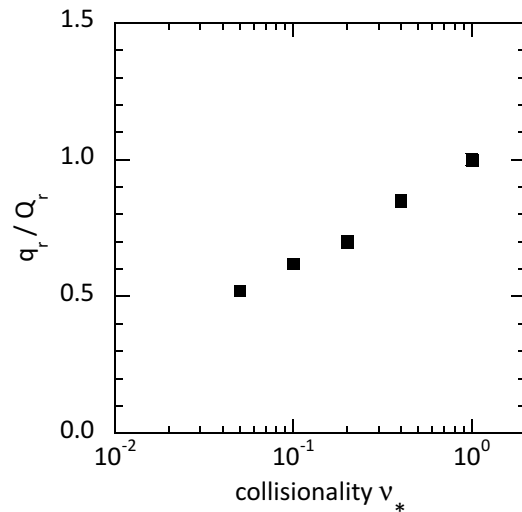


**Figure 6.** The ratio of the radial heat flux  $q_r$  to the radial energy flux  $Q_r$  depends on the collisionality  $\nu_*$  in the radially-bounded ergodic region, where the values of the fluxes are evaluated at  $r/a = 0.8$ . The radial energy transport becomes conductive as the collisionality increases,  $\nu_* \rightarrow 1$ , where  $Q_r = q_r + (5/2)T\Gamma_r$  and  $\Gamma_r$  is the radial particle flux. Note that in all cases,  $Q_r$  is positive and the temperature is set to be 0.955 keV.

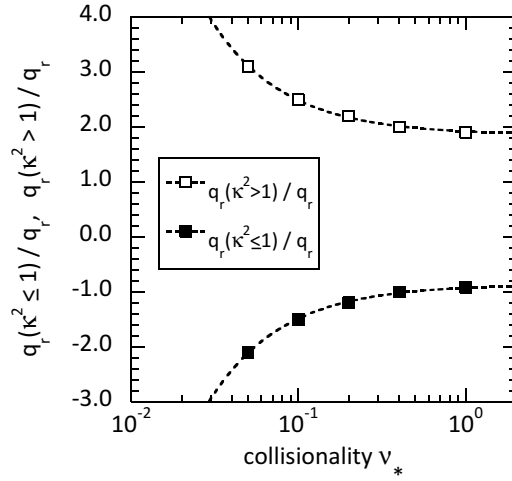


**Figure 7.** The contributions of untrapped and trapped particles to the radial heat flux,  $q_r(\kappa^2 > 1)/q_r$  and  $q_r(\kappa^2 \leq 1)/q_r$ , depend on the collisionality  $\nu_*$  in the radially-bounded ergodic region, as shown by the open and closed squares, respectively, where the values are evaluated at  $r/a = 0.8$  and  $\kappa^2$  is defined as  $\kappa^2 = \{(1/2)mv^2 - \mu B_{ax}(1 - \epsilon_t)\}/2\mu B_{ax}\epsilon_t$ . Note that  $q_r = q_r(\kappa^2 > 1) + q_r(\kappa^2 \leq 1)$  is positive in all cases. The regression curves are given by the dashed lines.